



Comparative Studies of Phonon Frequency Spectrum of HTSCs $GdBa_2Cu_3O_7$ and $SmBa_2Cu_3O_7$ Through Lattice Dynamics.

K.SONAMUTHU*, GEENA VIDYA . S

(*J N R Mahavidyalaya, Port Blair, South Andaman, India.744104
Sathyabamal Engineering College, Chennai-600066)

ABSTRACT

The prime application of Nano technology is High temperature superconductor. The normal state and superconducting properties are believed to arise from the strongly correlated motion of the electronic charge carries (electrons or holes) in the CuO_2 planes that essentially define the layered Cuprate HTSC. The other cations and oxygen atom in the structure provides structural stability and control the number of charge carries in the CuO_2 planes. The Raman spectroscopy of HTSC explains that the role played by the phonons in the mechanism of superconductivity in the perovskite family of superconductors is not fully understood although a large series of experimental results has shown considerable coupling of some phonons to electronic excitation in these systems. Optical spectroscopy and especially Raman and Infrared spectroscopy revealed strong direct influences of the changes in the electronic states to the phonon at the center of the Brillouin. The lattice dynamics method is suited to determine the phonon frequencies in the proximity of the Brillouin zone centre only. But, the force constants obtained from that analysis do not provide a stable dynamics throughout the Brillouin zone. However, it is indispensable to have a precise knowledge of the zone –boundary phonons to investigate the contribution of electron-phonon coupling to T_c which can be achieved by neutron scattering techniques. The most commonly employed model is the valence force field model for computing phonon frequencies based on stretching bond and bending bond coordinates. Such models have the advantage of being well adopted to describe a covalent bonding but ignored the long-range Coulomb forces and wave vector dependence of the phonon spectrum. This work considered only the $q=0$ modes and the number of model parameters exceeded the number of experimental data. The rigid ion model on the other hand considers both the short-range repulsive interactions and the long range Coulomb interaction among various rigid ions in the crystal..

Key words: Superconductor, Raman spectroscopy, Infrared symmetry, Brillouin, Three Body Force Shell Model, Phonon frequency, Lattice Dynamical Calculation, PED, etc.,

1. Introduction

The discovery of the high super conducting transition of the La-Ba-Cu-O system by Bednorz and Muller has caused unprecedented world wide activities in the search and characterization of high T_c superconductor is of importance, not only for the overall physical characterization of the role played by the phonons in the superconducting phenomenon. Born-Killermann theory of ionic crystals explains the temperature variation of specific heats of many alkali halides reasonable well, but falls to describe the details of vibrational spectra. The three body force shell model (TSM) developed from Verma and Singh [1-2] was reviewed by Cochran on the simple consideration that the electron shell is deformation. This deformation give rise to the three body interactions and accounts for

the observed Cauchy discrepancy. The displacement on the other hand introduces the electronic polarization and accounts for the dielectric properties. Veram and Agarwal [3] redefined the shell and core charges suitably and hence the basic equation of the model have been modified. Lundqvist et al. [4] has shown that TSM is equivalent to the breathing shell model (BSM).

2. Lattice Dynamics of HTSCs GdBa₂Cu₃O₇ and SmBa₂Cu₃O₇ based on Three Body Force Shell Model

The new high T_c materials contain numerous particles in the unit cell. Thus, in a classical approach to lattice dynamics, a large number of unknown force constants has to be specified. Much attention has been paid, from several points of view, to copper-oxide-based high T_c Superconductors with the formula GdBa₂Cu₃O₇ and SmBa₂Cu₃O₇ discovered by W.Kress et al. [5]. The study of the lattice dynamics of the high T_c Superconductors is of importance, not only for the overall physical characterization of these compounds, but also for an assessment of the role played by the phonons in the superconducting phenomenon. Our approach is based on the use of long-range Coulomb potentials and short-range repulsive Born Mayer potentials, as well as ionic polarizabilities, in the framework of the shell model [6-13].

The calculation of lattice dynamical vibration frequencies of GdBa₂Cu₃O₇ and SmBa₂Cu₃O₇ systems are performed by three-body force shell model (TSM) calculations. In the shell model calculation the equations of the motion for the core coordinate U and the shell coordinate are expressed as [14] follows:

$$\begin{aligned} -M \omega^2 U &= (R + ZC'Z) U + (T + ZC'Z) W \\ 0 &= (T - YC'Z) U + (S + K + YC'Y) W \end{aligned}$$

with $ZC'Z = Z [Z + 12 f(a)] C + V$ where M , Z and Y are diagonal matrices representing the mass ionic charge on the shell, R , S , T are matrices specifying short-range core-core, shell-shell and core-shell interactions respectively, V is the matrix describing the three-body overlap interactions and $f(a)$ is related to overlap integrals of electron wave function. U and W are the vectors describing the ionic displacements and deformations respectively.

In the earlier approaches the R , S and T elements were considered to be equal to one another. In the present investigation, we have started with an approach such that $R \neq S \neq T$ [15]. That is the various interactions between the ions are treated in a more general way without making them numerically equal. The dynamical matrix of the model consists of long-range Coulomb and three-body interactions and the short range overlap repulsions. The off-diagonal elements of this matrix along the symmetry directions chain a completely new term having a significant contribution for unequal R , S and T .

The lattice dynamical calculation of high-temperature superconductors is explained using an inter ionic potential consisting of long-range Coulomb part and a short range Potential of Born-Mayer form [16].

$$V_{ij} = a_{ij} \exp. (-b_{ij}. r)$$

Where i, j label the ions and r is their separation. The parameters a_{ij} and b_{ij} are the pair potentials and the parameters Y and K determine the electronic polarizabilities. The parameters used in the present calculations are given in Table 1. Phonon frequencies are calculated using the force constants derived from the inter ionic potential. Following Mohan, et al [17] inter-ionic pair potentials for short-rang interactions can be transferred from one structure to another in similar environments. The force constants evaluated by this method are in good agreement with the evaluated values [18-30]

3. Result and Discussion:

The lattice dynamics of high temperature of high temperature superconductors have been performed using rigid ion model. The modified three body shell model is adopted in the lattice dynamical study gives favourable phonon frequencies, which are given as shown below:

3.1 Comparative studies of Lattice Dynamical Calculations of HTSCs $GdBa_2Cu_3O_7$ and $SmBa_2Cu_3O_7$:

The Lattice Dynamical calculations based on modified TSM reproduce the observed frequencies of Raman and infrared active modes reasonable which are given in table 2. The calculated frequencies of both of the HTSCs $GdBa_2Cu_3O_7$ and $SmBa_2Cu_3O_7$ are in good agreement with the available experimental values are proved at various symmetries.

The lowest calculated phonon frequencies of both of the HTSCs $GdBa_2Cu_3O_7$ and $SmBa_2Cu_3O_7$ in A_{1g} symmetry are at 165 cm^{-1} and 140 cm^{-1} are due to the vibration of Gd and Sm atoms respectively and these calculated frequencies agrees very well with the experimental frequencies at 162 cm^{-1} and 115 cm^{-1} respectively. Similarly the calculated phonon Raman frequencies of HTSC $GdBa_2Cu_3O_7$ in A_{1g} symmetry are at 325 cm^{-1} , 420 cm^{-1} and 436 cm^{-1} are due to the vibrations of Ba,Cu and O(2) atoms respectively and the calculated Raman frequencies of HTSC $SmBa_2Cu_3O_7$ in A_{1g} symmetry are at 220 cm^{-1} , 420 cm^{-1} and 440 cm^{-1} are due to the vibrations of Ba,Cu and O(2) atoms respectively. Similarly, the observed Raman frequencies of HTSC $GdBa_2Cu_3O_7$ in A_{1g} symmetry are at 320 , 425 and 435 cm^{-1} and the observed Raman frequencies of frequencies of HTSC $SmBa_2Cu_3O_7$ in A_{1g} symmetry are at 215 cm^{-1} , 420 cm^{-1} and 445 cm^{-1} agrees very well with the calculated frequencies respectively. The highest calculated Raman frequencies of both of the HTSCs $GdBa_2Cu_3O_7$ and $SmBa_2Cu_3O_7$ in A_{1g} symmetry are at 555 cm^{-1} each are due to the vibration of O(2) atom each. Here, the observed frequencies of both of the HTSCs are at 550 cm^{-1} agrees very well with the calculated frequency at 555 cm^{-1} each respectively which is confirmed by the PED calculation

The lowest calculated phonon frequencies of both of the HTSCs $GdBa_2Cu_3O_7$ and $SmBa_2Cu_3O_7$ in B_{2g} symmetry are at 150 cm^{-1} and 90 cm^{-1} are due to the vibration of Gd and Sm atoms respectively and these calculated frequencies agrees very well with the experimental frequencies at 145 cm^{-1} and 80 cm^{-1} respectively. Similarly the calculated phonon Raman frequencies of HTSC $GdBa_2Cu_3O_7$ in B_{2g} symmetry are at 310 cm^{-1} , 470 cm^{-1} and 545 cm^{-1} are due to the vibrations of Ba,Cu and O(2) atoms respectively and the calculated Raman frequencies of HTSC $SmBa_2Cu_3O_7$ in B_{2g} symmetry are at 140 cm^{-1} , 482 cm^{-1} and 587 cm^{-1} are due to the vibrations of Ba,Cu and O(2) atoms respectively. Similarly, the observed Raman frequencies of HTSC $GdBa_2Cu_3O_7$ in B_{2g} symmetry are at 320 , 480 and 550 cm^{-1} and the observed Raman frequencies of frequencies of HTSC $SmBa_2Cu_3O_7$ in A_{1g} symmetry are at 150 cm^{-1} , 480 cm^{-1} and 587 cm^{-1} agrees very well with the calculated frequencies respectively. The highest calculated Raman frequencies of both of the HTSCs $GdBa_2Cu_3O_7$ and $SmBa_2Cu_3O_7$ in B_{2g} symmetry are at 570 cm^{-1} and 637 cm^{-1} are due to the vibration of O(2) atom each. Here, the highest observed phonon frequencies of both of the HTSCs $GdBa_2Cu_3O_7$ and $SmBa_2Cu_3O_7$ in B_{2g} symmetry are at 580 cm^{-1} and 630 cm^{-1} are due to the vibration of O(3) atoms each and these observed frequencies agree very well with the calculated frequencies at 570 cm^{-1} and 637 cm^{-1} respectively, which is confirmed by the PED calculation.

The lowest calculated phonon frequencies of both of the HTSCs $GdBa_2Cu_3O_7$ and $SmBa_2Cu_3O_7$ in B_{3g} symmetry are at 114 cm^{-1} and 77 cm^{-1} are due to the vibration of Gd and Sm atoms respectively and these calculated frequencies agrees very well with the experimental frequencies at 110 cm^{-1} and 78 cm^{-1} respectively. Similarly the calculated phonon Raman frequencies of HTSC $GdBa_2Cu_3O_7$ in B_{3g} symmetry are at 290 cm^{-1} , 572 cm^{-1} and 578 cm^{-1} are due to the vibrations of Ba,Cu and O(2) atoms respectively and the calculated Raman frequencies of HTSC $SmBa_2Cu_3O_7$ in B_{2g} symmetry are at 125 cm^{-1} , 560 cm^{-1} and 580 cm^{-1} are due to the vibrations of Ba,Cu and O(2) atoms respectively. Similarly, the observed Raman frequencies of HTSC $GdBa_2Cu_3O_7$ in B_{3g} symmetry are at 270 , 565 and 580 cm^{-1} and the observed Raman frequencies of frequencies of HTSC $SmBa_2Cu_3O_7$ in B_{3g} symmetry are at 127 cm^{-1} , 560 cm^{-1} and 570 cm^{-1} agrees very well with the calculated frequencies respectively. The calculated Raman frequencies of both of the HTSCs $GdBa_2Cu_3O_7$ and $SmBa_2Cu_3O_7$ in B_{3g} symmetry are at 638 cm^{-1} and 640 cm^{-1} are due to the vibration of O(2) atom each. Here, the highest observed phonon frequencies of both of the HTSCs $GdBa_2Cu_3O_7$ and $SmBa_2Cu_3O_7$

in B_{3g} symmetry are at 640 cm^{-1} and 625 cm^{-1} are due to the vibration of O(3) atoms each and these observed frequencies agree very well with the calculated frequencies at 638 cm^{-1} and 640 cm^{-1} respectively, which is confirmed by the PED calculation.

The evaluated Infrared (IR) phonon frequencies of HTSC $\text{GdBa}_2\text{Cu}_3\text{O}_7$ in B_{1u} symmetry are at 122 cm^{-1} and 180 cm^{-1} are due to the vibration of Gd and Ba atoms respectively, whereas the evaluated Infrared (IR) phonon frequencies of HTSC $\text{SmBa}_2\text{Cu}_3\text{O}_7$ in B_{1u} symmetry are at 88 cm^{-1} and 190 cm^{-1} are due to the vibration of Sm and Ba atoms respectively. The observed Infrared (IR) phonon frequencies in B_{1u} symmetry of HTSC $\text{GdBa}_2\text{Cu}_3\text{O}_7$ are at 120 cm^{-1} and 180 cm^{-1} and in HTSC $\text{SmBa}_2\text{Cu}_3\text{O}_7$ the experimental frequencies are at 80 cm^{-1} and 190 cm^{-1} which agrees very well with the calculated frequencies of both of the superconductors. The Calculated infrared phonon frequency of HTSC $\text{GdBa}_2\text{Cu}_3\text{O}_7$ at 275 cm^{-1} and the Calculated infrared phonon frequency of HTSC $\text{GdBa}_2\text{Cu}_3\text{O}_7$ at 225 cm^{-1} in B_{1u} symmetry is due to the vibration of Cu(1) atoms. Similarly, the Calculated infrared phonon frequency of HTSC $\text{GdBa}_2\text{Cu}_3\text{O}_7$ at 225 cm^{-1} in B_{1u} symmetry is due to the vibration of Cu(1) atom, The observed frequencies of both of the HTSCs $\text{GdBa}_2\text{Cu}_3\text{O}_7$ and $\text{SmBa}_2\text{Cu}_3\text{O}_7$ are at 270 cm^{-1} and 250 cm^{-1} agrees very well with the calculated frequencies respectively. The IR frequencies' at 415 cm^{-1} , 485 cm^{-1} and 500 cm^{-1} of HTSC $\text{GdBa}_2\text{Cu}_3\text{O}_7$ are due to the vibration of Cu(2), O(1) and O(2) atoms respectively, whereas the IR frequencies at 415 cm^{-1} , 485 cm^{-1} , and 500 cm^{-1} of HTSC $\text{SmBa}_2\text{Cu}_3\text{O}_7$ are due to the vibration of Cu(2), O(1) and O(2) atoms respectively and the observed IR frequency of HTSC $\text{GdBa}_2\text{Cu}_3\text{O}_7$ are at 420 cm^{-1} , 480 cm^{-1} and 510 cm^{-1} and the observed IR frequency of HTSC $\text{SmBa}_2\text{Cu}_3\text{O}_7$ at 419 cm^{-1} , 480 cm^{-1} and 575 cm^{-1} agrees very well with the calculated frequencies. The highest calculated IR phonon frequencies of both of the HTSCs $\text{GdBa}_2\text{Cu}_3\text{O}_7$ and $\text{SmBa}_2\text{Cu}_3\text{O}_7$ in B_{1u} symmetry are at 648 cm^{-1} and 630 cm^{-1} are due to the vibration of O(3) atoms each and the observed frequencies of HTSCs $\text{GdBa}_2\text{Cu}_3\text{O}_7$ and $\text{SmBa}_2\text{Cu}_3\text{O}_7$ are at 650 cm^{-1} and 630 cm^{-1} respectively agrees very well with the calculated frequencies, which is confirmed by the PED calculation.

The calculated Infrared phonon frequencies of HTSC $\text{GdBa}_2\text{Cu}_3\text{O}_7$ in B_{2u} symmetry are at 648 cm^{-1} , and 635 cm^{-1} are due to the vibrations of O(2) and O(3) atoms respectively and the calculated Infrared frequencies of HTSC $\text{SmBa}_2\text{Cu}_3\text{O}_7$ in B_{2u} symmetry are at 612 cm^{-1} and 635 cm^{-1} are due to the vibrations of O(2) and O(3) atoms respectively. Similarly, the observed IR frequencies of HTSC $\text{GdBa}_2\text{Cu}_3\text{O}_7$ in B_{2u} symmetry are at 620 cm^{-1} and 630 cm^{-1} and the observed IR frequencies of HTSC $\text{SmBa}_2\text{Cu}_3\text{O}_7$ in B_{2u} symmetry are at 610 cm^{-1} and 630 cm^{-1} agrees very well with the calculated frequencies respectively which is confirmed by the PED calculation.

The calculated IR frequency of HTSC $\text{GdBa}_2\text{Cu}_3\text{O}_7$ in E_u symmetry at 118 cm^{-1} is due to the vibration of Gd atom and its observed phonon frequency is at 118 cm^{-1} and this observed frequency agrees very well with the calculated frequency. The calculated IR frequencies at 195 cm^{-1} , 212 cm^{-1} and 572 cm^{-1} are due to the bending bond vibration of Ba, Ca, and O(1) atoms respectively and its corresponding observed phonon frequencies are at 180 cm^{-1} , 212 cm^{-1} and 560 cm^{-1} agrees very well with the calculated frequencies. The highest calculated IR phonon frequency at 580 cm^{-1} is due to the vibration of O(3) atom which performs stretched bending bond vibration and its observed frequency is at 575 cm^{-1} and it agrees very well with the calculated frequency. Similarly, The calculated IR frequencies of HTSCs $\text{SmBa}_2\text{Cu}_3\text{O}_7$ in E_u symmetry at 87 cm^{-1} is due to the vibration of Sm atom and its observed phonon frequency is at 86 cm^{-1} and these observed frequency agrees very well with the calculated frequency. The calculated IR frequencies at 172 cm^{-1} , 190 cm^{-1} and 555 cm^{-1} are due to the bending bond vibration of Ba, Ca, and O(1) atoms respectively and its corresponding observed phonon frequencies are at 180 cm^{-1} , 189 cm^{-1} and 556 cm^{-1} respectively agrees very well with the calculated frequencies. The highest calculated IR phonon frequency at 585 cm^{-1} is due to the vibration of O(3) atom which performs stretched bending bond vibration and its observed frequency is at 587 cm^{-1} and it agrees very well with the calculated frequency. Therefore, the calculated and observed frequencies of both of the HTSCs $\text{GdBa}_2\text{Cu}_3\text{O}_7$ and $\text{SmBa}_2\text{Cu}_3\text{O}_7$ agrees very well with each other which is confirmed by the PED calculation.

The calculated IR frequency of HTSC $\text{GdBa}_2\text{Cu}_3\text{O}_7$ in B_{3u} symmetry at 180 cm^{-1} is due to the vibration of Gd atom and its observed phonon frequency is at 175 cm^{-1} and this observed frequency agrees very well with the calculated frequency. The calculated IR

frequencies at 190 cm^{-1} , 450 cm^{-1} , 535 cm^{-1} and 576 cm^{-1} are due to the bending bond vibration of Ba, Cu, and O(1) and O(2) atoms respectively and it corresponding observed phonon frequencies are at 180 cm^{-1} , 420 cm^{-1} , 540 cm^{-1} and 580 cm^{-1} which agrees very well with the calculated frequencies. The highest calculated IR phonon frequency in this symmetry at 640 cm^{-1} is due to the vibration of O(3) atom which performs starched bending bond vibration and its observed frequency is at 635 cm^{-1} and it agrees very well with the calculated frequency. Similarly, The calculated IR frequencies of HTSCs $\text{SmBa}_2\text{Cu}_3\text{O}_7$ in B_{3u} symmetry at 150 cm^{-1} is due to the vibration of Sm atom and its observed phonon frequency is at 145 cm^{-1} and these observed frequency agrees very well with the calculated frequency. The calculated IR frequencies in this symmetry at 193 cm^{-1} , 463 cm^{-1} , 523 cm^{-1} and 584 cm^{-1} are due to the bending bond vibration of Ba, Ca, O(1) and O(2) atoms respectively and its corresponding observed phonon frequencies are at 196 cm^{-1} , 465 cm^{-1} , 520 cm^{-1} and 584 cm^{-1} respectively agrees very well with the calculated frequencies. The highest calculated IR phonon frequency in this symmetry at 650 cm^{-1} is due to the vibration of O(3) atom which performs starched bending bond vibration and its observed frequency is at 665 cm^{-1} which agrees very well with the calculated frequency. Therefore, the calculated and observed frequencies of both of the HTSCs $\text{GdBa}_2\text{Cu}_3\text{O}_7$ and $\text{SmBa}_2\text{Cu}_3\text{O}_7$ agrees very well with each other which is confirmed by the PED calculation.

4. Conclusion:

In this present investigation, the Comparative Studies of Phonon Frequency Spectrum of HTSCs $\text{GdBa}_2\text{Cu}_3\text{O}_7$ and $\text{SmBa}_2\text{Cu}_3\text{O}_7$ Through Lattice dynamical calculations yield the same phonon frequencies behaves as the bridge between Solid State Physics and Spectroscopy to understand the mechanism of superconductivity. The Raman and infrared studies of these HTSC have contributed significantly to their understanding. The assignment of the spectral features to specific lattice vibrations would be an important step in understanding their role in superconductivity.

In this work the lattice dynamics technique have been adopted to give the evidence for electron, phonon interaction in HTSCs $\text{GdBa}_2\text{Cu}_3\text{O}_7$ and $\text{SmBa}_2\text{Cu}_3\text{O}_7$. It is observed from the tables that the agreement between the calculated and observed frequencies were in good agreement with the systems that are considered here. This fact supports that the present vibrational assignments made for the infra red and Raman spectra are adequate. Therefore it is concluded that the lattice dynamics is the optically active vibrations of the vibrational spectra in cuprate oxides.

Therefore, the lattice dynamics calculations yielded not only by the zone center phonon modes but also by the stable dispersions. Hence, it also supports the strong electron phonon interaction in high temperature super conductor (HTSC). The vibrational frequencies calculated by the method of lattice dynamics are compared theoretically and experimentally, and they appears to be in good agreement that are further confirmed by the potential energy distribution calculation.

Lastly, it is concluded that metal – oxide (Cu-O) plays an important role for the occurrence of superconductivity. The Raman scattering has provided direct evidence for strong electron –phonon interaction in the high T_c superconducting oxides. The vibrational frequencies calculated by the methods of Lattice Dynamics are compared and they appears to be in good agreement, which is confirmed by the Potential Energy Distribution calculation..

5. Reference:

- [1] M.P. Verma, R.K. Singh, Phys. Stat. Sol. 33 (1969) 769.
- [2] M.P. Verma, R.K. Singh, J. Phys. C 4 (1971) 2745.
- [3] M.P. Verma, S.K. Agarwal, Phys. Rev. B (1973) 4880.
- [4] S.O. Lundqvist, Ark. Fysik 9 (1955) 435.
- [5] W. Kress, U. Schorder, J. Prade, A.D. Kulkarni, F.W. de Watte, Phys. Rev. B 38 (1988) 2906.
- [6] J.G. Bednorz and K.A. Muller, Z.Phys. B64 (1986) 189.
- [7] P.H. Hor et al., Phys. Rev. Lett. 58, (1987) 1891.
- [8] G. Xiao et al., Phys. Rev. B35, (1987) 8782.
- [9] Y.K. Atanassova, V.N. Popov, G.G. Bogachev, M.N. Iiiev, C. Mitros,
- [10] V. Psychais, and M. Pissas, Phys. Rev. B47 (1993) 15201.
- [11] E.B. Wilson Jr, J.C. Decius and P.C. Cross, Molecular vibrations, Mc Graw Hill, New York (1955).
- [12] T. Shimanouchi, M. Tsuboi and T. Miyazawa, J. Chem. Phys. 35 (1961) 1597.
- [13] S. Mohan and A. Sudha, Pramana-J. Phys 37 (1991) 327.
- [14] H. Fuhrer, V.B. Kartha, K.L. Kidd, P.J. Kruger and H.H. Mantsch, Computer program for Infrared

and spectrometry, Normal coordinate analysis, vol. 5, National Research Council, Ottawa, Canada (1976).

- [15] S. Mohan and K. Sonamuthu, Phys. Stat. Solidi. B 229 (2002) 1121. Solid State Science and Technology, Vol. 13, No 1 & 2 (2005) 276-286 ISSN 0128-7389 286
- [16] S. Mohan and K. Sonamuthu, Physica B, 321 [2002]342.
- [17] S. Mohan and A. Sudha, Vibrational spectroscopy (Elsevier) 3 (1992) 79
- [18] Rudolf Fene, Physica C 159, (1989)1.
- [19] W. Kress et al, Physica C 162-164, (1989) 1345.
- [20] S. Onari et al, Solid State Commun 71(1989) 195.
- [21] J. Prade et al, Phy. Rev B 39 (1989)2771.
- [22] K.K. Yim et al, Solid State Commun 77 (1991)385.
- [23] S. Mohan and R. Kannan, Aust. J. Phys, 47 (1994)103
- [24] S. Mohan, S. Durai and G. Vaidyanathan, Ind. J. Phys, A60 [1986] 137
- [25] E. W. Kellermann, Phil. Trans Roy. Soc. Land, A238 [1940] 513
- [26] S. Mohan and A. Sudha, Indian. J. Pure & Appl. Phys, 31 (1993)57
- [27] S. Mohan and C. Vasantha, Proc. Indian. Natn. Sci. Acad. 58a (1992) 107.
- [28] S. Mohan, R. Kannan and G. Vaidyanathan, Proc. Nat. Acad. Sci, 62A(1992) 1.
- [29] S. Mohan, Mod. Phys. Letts B 3 (1989)115
- [30] A.D.Kulkarni and F.W.de Watte, J.Prade and U.Schroder W.Kress, Phys. Rev. B39(1989)2771.

Table: 1

Force constants for HTSCs of $GdBa_2Cu_3O_7$ and $SmBa_2Cu_3O_7$

Parameters of the model: a, b are Born-Mayer constants: Z,Y,K, ionic charge, shell charge and on-site core-shell force constant of the ion, V_a is the volume of the unit cell.

Force constants for $GdBa_2Cu_3O_7$			Force constants for $SmBa_2Cu_3O_7$		
Interaction	a (eV)	b (\AA^{-1})	Interaction	a (eV)	b (\AA^{-1})
Gd-O	3100	2.80	Sm-O	3200	2.80
Ba-O	3225	3.55	Ba-O	3225	3.55
Cu-O	1260	3.35	Cu-O	1260	3.22
O-O	1000	3.00	O-O	1000	3.00

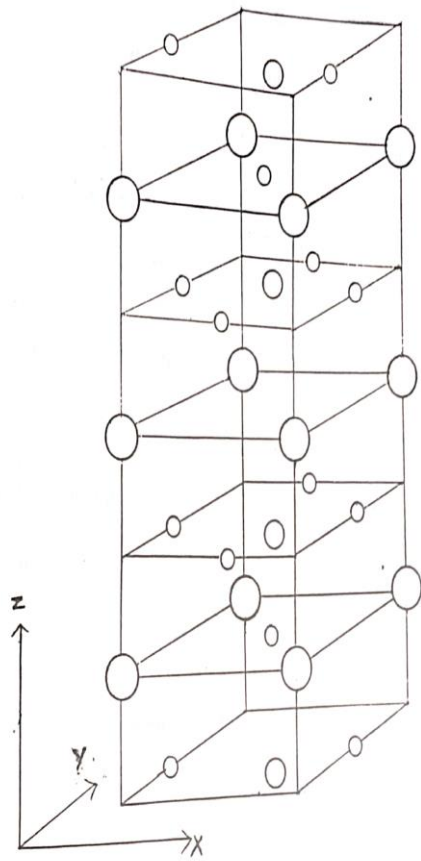
$GdBa_2Cu_3O_7$				$SmBa_2Cu_3O_7$			
Ion	Z(e)	(e)	$k(e^2 Va)$	Ion	Z(e)	(e)	$k(e^2 Va)$
Gd	2.61	2.90	985	Sm	2.61	2.90	895
Ba	1.90	2.32	179	Ba	1.91	2.32	179
Cu	1.80	3.22	135	Cu	1.80	3.22	135
O (Cu-O)	-1.81	-2.70	252	O (Cu-O)	-1.81	-2.70	252
O (Cu-O)	-1.81	-2.70	252	O (Cu-O)	-1.81	-2.70	252
O(Ba-O)	-1.93	-2.70	310 (K) 2100(K _⊥)	O(Ba-O)	-1.93	-2.70	310 (K) 2100(K _⊥)

$GdBa_2Cu_3O_7$			$SmBa_2Cu_3O_7$		
Interaction	A($e^2/2Va$)	B($e^2/2Va$)	Interaction	A($e^2/2Va$)	B($e^2/2Va$)
Cu-O(2)	576	-90.8	Cu-O(2)	576	-90.8
Gd-O(2)	563	-80.5	Sm-O(2)	530	-80..0
Ba-O(2)	114	-13.2	Ba-O(2)	114	-13.2
O(3) -O(2)	62	-7.5	O(3) -O(2)	62	-7.5

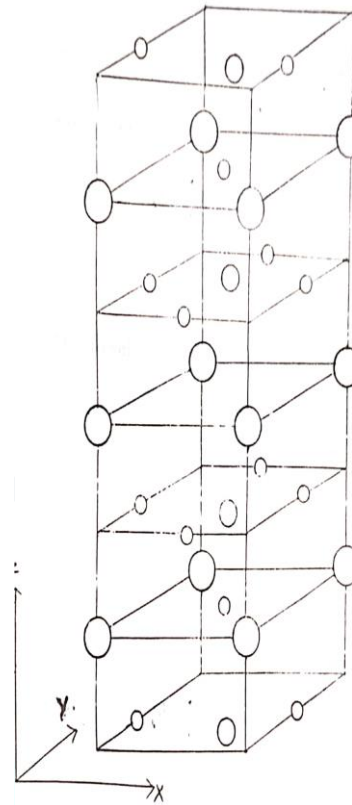
Table: 2.

Calculated Phonon frequencies of $GdBa_2Cu_3O_7$ and $SmBa_2Cu_3O_7$ *(Values in the Parentheses are experiment frequencies.)*

Symmetry species	Frequency(cm^{-1}) Lattice Dynamics of $GdBa_2Cu_3O_7$	Frequency(cm^{-1}) Lattice Dynamics Of $SmBa_2Cu_3O_7$	Potential Energy Distribution(%) $GdBa_2Cu_3O_7$	Potential Energy Distribution(%) $SmBa_2Cu_3O_7$
A_{1g} (Raman)	555(550)	555(550)	$f_b(70)f_e(10)$	$f_b(76)f_e(12)$
	436(435)	440(445)	$f_l(50)f_k(20)$	$f_l(55)f_k(26)$
	420(425)	420(420)	$f_k(50)f_n(21)$	$f_k(54)f_n(21)$
	325(320)	220(215)	$f_p(60)f_a(18)f_e(15)$	$f_p(65)f_a(28)f_e(11)$
	165(162)	140(115)	$f_g(64)f_i(20)$	$f_g(68)f_i(21)$
B_{2g}	570(580)	637(630)	$f_c(52)f_m(35)f_p(18)$	$f_c(57)f_m(30)f_p(17)$
	545(550)	587(584)	$f_c(70)$	$f_c(72)$
	470(480)	482(480)	$f_h(58)$	$f_h(59)$
	310(320)	140(150)	$f_p(70)f_g(25)$	$f_p(67)f_g(24)$
	150(145)	90(80)	$f_g(60)f_n(20)$	$f_g(65)f_n(28)$
B_{3g}	638(640)	640(625)	$f_c(59)f_a(20)$	$f_c(58)f_a(20)$
	578(580)	580(570)	$f_c(84)$	$f_c(74)$
	572(565)	560(560)	$f_h(90)$	$f_h(89)$
	290(270)	125(127)	$f_p(50)f_i(19)$	$f_p(55)f_i(20)$
	114(110)	77(78)	$f_g(54)f_m(30)f_i(15)$	$f_g(54)f_m(28)f_i(11)$
B_{1u} (IR)	648(650)	630(630)	$f_b(50)f_p(20)f_m(20)$	$f_b(56)f_p(20)f_m(12)$
	500(510)	580(575)	$f_b(71)f_p(17)$	$f_b(67)f_p(18)$
	485(480)	475(480)	$f_k(50)f_a(11)$	$f_k(55)f_a(11)$
	415(420)	420(419)	$f_n(51)f_k(20)f_m(15)$	$f_n(58)f_k(24)f_m(14)$
	275(270)	225(250)	$f_c(64)f_b(20)$	$f_c(65)f_b(23)$
	180(180)	190(180)	$f_l(53)f_k(20)$	$f_l(60)f_k(21)$
	122(120)	88(80)	$f_a(64)f_p(32)f_g(10)$	$f_a(68)f_p(30)f_g(14)$
B_{2u}	635(630)	635(630)	$f_p(48)f_c(30)f_m(20)$	$f_p(58)f_c(20)f_m(12)$
	628(620)	612(610)	$f_a(78)f_g(15)$	$f_a(70)f_g(17)$
E_u	580(575)	585(587)	$f_a(85)$	$f_a(75)$
	572(560)	555(556)	$f_h(42)f_c(20)f_a(12)$	$f_h(52)f_c(28)f_a(15)$
	212(212)	190(189)	$f_a(68)f_h(30)$	$f_a(69)f_h(23)$
	195(180)	172(180)	$f_m(70)f_p(20)$	$f_m(67)f_p(25)$
	118(118)	87(86)	$f_k(68)f_a(15)$	$f_k(65)f_a(25)$
B_{3u}	640(635)	650(665)	$f_p(41)f_n(28)f_c(20)$	$f_p(51)f_n(30)f_c(11)$
	576(580)	584(570)	$f_c(70)f_m(20)$	$f_c(69)f_m(24)$
	535(540)	523(520)	$f_h(78)$	$f_h(72)$
	450(420)	463(465)	$f_g(78)f_r(21)$	$f_g(75)f_r(22)$
	190(180)	193(196)	$f_\gamma(82)$	$f_\gamma(72)$
	180(175)	150(145)	$f_n(58)f_p(30)$	$f_n(68)f_p(23)$



○ Gd, Ba
○ Cu
○ ○



○ Sm, Ba
○ Cu
○ ○

Fig.1 Crystal Structure of GdBa₂Cu₃O₇

Fig.2 Crystal Structure of GdBa₂Cu₃O₇